2018

Feasibility of Using an Equilibrium Point Strategy to Control Reaching Movements of Paralyzed Arms with Functional Electrical Stimulation

Matthew Huffman
Clevleand State University

FEASIBILITY OF USING AN EQUILIBRIUM POINT STRATEGY TO CONTROL REACHING MOVEMENTS OF PARALYZED ARMS WITH FUNCTIONAL ELECTRICAL STIMULATION

MATTHEW P. HUFFMAN

Bachelor of Science in Chemical Engineering

Cleveland State University

May 2015

submitted in partial fulfillment of requirements for the degree

MASTER OF SCIENCE IN BIOMEDICAL ENGINEERING

at the

CLEVELAND STATE UNIVERSITY

May 2018

We hereby approve this thesis for

Matthew P. Huffman

Candidate for the Master of Science in Biomedical Engineering degree for the

Department of Chemical and Biomedical Engineering

and the CLEVELAND STATE UNIVERSITY

College of Graduate Studies

____

Thesis Chairperson, Dr. Eric Schearer

____

Department & Date

____

Thesis Committee Member, Dr. Dan Simon

____

Department & Date

____

Thesis Committee Member, Dr. Antonie van den Bogert

____

Department & Date

Student’s Date of Defense: March 20, 2018

ACKNOWLEDGEMENT

I would first like to thank my thesis advisor Dr. Eric Schearer of the Mechanical Engineering Department at Cleveland State University. He consistently pushed me to think abstractly and allowed this thesis to be my own work, but continued to be a helping hand whenever he thought I needed it.

I would also like to thank the expert who was involved in the initial development of the modeling and coding software: Dr. Antonie van den Bogert of the Mechanical Engineering Department. Without his passion and professional input at all times, the modeling software could not have been successfully created.

I would also like to acknowledge student Titus Lungu of the Mechanical Engineering Department at Cleveland State University as a contributor to the initial research, and I am gratefully indebted to him for his valuable comments on this thesis.

FEASIBILITY OF USING AN EQUILIBRIUM POINT STRATEGY TO CONTROL REACHING MOVEMENTS OF PARALYZED ARMS WITH FUNCTIONAL ELECTRICAL STIMULATION

MATTHEW P. HUFFMAN

ABSTRACT

Functional electrical stimulation (FES) is a technology capable of improving the quality of life for those with the loss of limb movement related to spinal cord injuries. Individuals with high-level tetraplegia, in particular, have lost all movement capabilities below the neck. FES has shown promise in bypassing spinal cord damage by sending electrical impulses directly to a nerve or muscle to trigger a desired function. Despite advancements in FES, full-arm reaching motions have not been achieved, leaving patients unable to perform fundamental tasks such as eating and grooming.

To overcome the inability in current FES models to achieve multi-joint coordination, a controller utilizing muscle activations to achieve full-arm reaching motions using equilibrium point control on a computer-simulated human arm was developed. Initial simulations performed on the virtual arm generated muscle activations and joint torques required to hold a static position. This data was used as a model for Gaussian Process Regression to obtain muscle activations required to hold any desired static position. The accuracy of the controller was tested on twenty joint positions and was capable of holding the virtual arm within a mean of 1.1 ± 0.13 cm from an original target position.

Once held in a static position, external forces were introduced to the simulation to evaluate if muscle activations returned the arm towards the original position after being moved away within a basin of attraction. It was found that the basin of attraction was limited to a 15 cm sphere around the joint position, regardless of position in the workspace. Muscle activations were then tested and found to successfully perform movements between points within the basin. The development of a controller capable of equilibrium point controlled movement is the initial step in recreating these movements in high-level tetraplegia patients with an implanted FES.

TABLE OF CONTENTS

LIST OF TABLES

LIST OF FIGURES

CHAPTER I

INTRODUCTION

Spinal cord injuries (SCI) affect over 282,000 people in the United States alone (National Spinal Cord Injury Statistical Center, 2017). Of these individuals, 58.3% have some level of tetraplegia - an injury that results in the partial or total loss of movement in all four limbs and torso - while 41.7% have some degree of paraplegia - an injury that results in the partial or complete loss of the movement of the lower body (National Spinal Cord Injury Statistical Center, 2017). Loss of movement occurs because an injury to the spinal cord disrupts the proper communication channels of electrical impulses from the brain to the rest of the body. Individuals who have an injury anywhere below the C4 vertebrae have some functional ability in their arms and shoulders and can potentially lead an independent lifestyle, as they require help only with fine finger movements and larger muscle group movement. However, the most severe level of spinal cord injury that can occur is high-level tetraplegia - an injury to the spinal cord that occurs anywhere between the C1 to C4 vertebrae - which results in the complete loss of any movement below the neck, including the shoulders. These individuals require the highest level of care as they are unable to utilize any motion in their arms, leaving them completely dependent on others for daily activities such as eating and grooming. We aim to restore functional reaching in individuals with high-level tetraplegia as it is considered their highest priority as current methods are lacking in these advances (Anderson, 2004).

A vital aspect of improving the quality of life for those who live with high-level tetraplegia is attempting to supplement nonfunctioning muscles to regain some level of movement or functionality. One method that attempts to bridge the communication gap to support restoration of movement is Functional electrical stimulation (FES), a technique that applies small independent electrical impulses to paralyzed muscles to restore or improve their function (Ho, 2014). When only one or very few muscles or nerves were stimulated in various spinal cord injury patients across multiple studies, FES successfully restored and improved hand functionality (Keith, 1996), lower limb functions (Zhang, 2007), respiratory functions (Jarosz, 2012), and even bowel and bladder functions (Ho, 2014). Additionally, FES electrodes placed on various areas of the body for recurrent physical therapy have been shown to reduce common physiological problems associated with the loss of supraspinal control of voluntary movements such as increased body fat, leg edema, blood clots, decreased muscle bulk and endurance, pressure ulcers, osteoporosis, and depression (Ho, 2014).

Research focused on sending electrical impulses to damaged arm muscles utilizing FES has been promising in single-joint and coordinated multi-joint arm movements, but limited due to the complexity of the arm and shoulder system (Ajiboye, 2017). The complex structure of the human arm and the necessity for several joints and large muscle groups to be stimulated to achieve movement leaves FES less successful when attempting full-arm reaching movements. The most recent successes in FES-controlled full-arm reaching are the MUNDUS project (Pedrocchi, 2013) and the

Braingate clinical trial (Ajiboye, 2017), both of which have significantly improved the subject's abilities in laboratory demonstrations to perform everyday activities such as picking up a cup and reaching towards objects by the direct training of a controller specifically for these tasks. The MUNDUS project achieves joint motion by controlling a single degree of freedom at a time while an exoskeleton locks the other motions (Pedrocchi, 2013). However, the MUNDUS project does not exploit the redundancy of the arm to achieve different paths to the same target or modulate stiffness, limiting the flexibility of the tasks to be achieved. The Braingate clinical trial uses an intracortical brain-computer interface combined with FES to cortically command single-joint and coordinated multi-joint arm movements for point-to-point target acquisitions (Ajiboye, 2017). Despite the Braingate's advances, it currently lacks efficient control of multi-joint movements. The Braingate uses a fixed muscle activation pattern for flexion and extension of each independent joint and when attempting to control more than one joint at a time, the activation pattern of one joint conflicts with the others (Ajiboye, 2017). Furthermore, it uses an exoskeleton to control the shoulder, separating the shoulder and elbow into separate units and allowing only muscles below the shoulder to have freedom of movement. Developing a method of upper limb movement that can exploit the redundancy of the arm and control the shoulder and elbow as one unit outside of a laboratory would overcome the current disadvantages in the most modern FES systems as they rely on separating the shoulder and elbow into separate units to train a controller.

With full-arm reaching yet to be realized, patients with high tetraplegia are unable to completely utilize full motion of their arms to perform simple tasks such as holding a fork or brushing their hair. To restore movement and functions similar to what they were pre-injury, an individual must be able to attain any goal-directed task by being able to move their arm anywhere within their field of movement. However, the sheer number of possible goal tasks makes direct training of a controller to meet each goal improbable. Therefore, there exists a need for the development of a controller which can determine the stimulation commands necessary to achieve any desired task.

We hypothesized that equilibrium point control is one appropriate method to achieve this goal. We intend to use the same basic principles of the Equilibrium Point Hypothesis by determining which muscle groups to activate to achieve a given static equilibrium position and then attempt movements between these static positions. Equilibrium point control requires less strict direct training of a controller compared to the other research methods and instead can categorize movements into transitions between equilibrium points. This research uses the objectives below to develop a method capable of full-arm reaching movements through equilibrium point control of muscle activation in a computer-simulated human arm model. We aim to implement this research into an FES neuroprosthesis implanted in an individual with high-level tetraplegia to attempt to replicate the successes of the computer-simulated model into that of an actual patient with high tetraplegia. To test this hypothesis, our research focused on three main objectives:

1. Determine if muscle activations can maintain holding for static positions
2. Determine the existence and size of the basin of attraction around static positions
3. Determine the feasibility of changing muscle activations to move between static positions

We focused our research on a computer-simulated virtual human arm model developed to mimic a physical arm's response to muscle activation and output static and dynamic arm data (Chadwick, 2014). The success of the equilibrium point control strategy would give us confidence in its achievements in later experiments in human subjects. The controller was used to determine open-loop activation inputs to achieve a variety of arbitrary static hand positions. Gaussian Process Regression then utilized the static arm data to estimate joint dynamics and muscle activations necessary to achieve any specified static position within the field of movement. The feasibility of maintaining static positions allowed for further examination of movements between static points along a trajectory. The method of movement between static equilibrium points is the fundamental basis of the Equilibrium Point Hypothesis – the idea that the body moves equilibrium points which triggers shifting of the equilibrium point of the arm and generates movement (Feldman, 1986).

For individuals with high tetraplegia, the loss of purposeful motion in their upper extremities severely limits their quality of life, and restoring this functionality is their greatest priority to improving their independence (Anderson, 2004). Refining the accuracy of full-arm reaching movements can significantly increase the number of functional tasks they could perform and decrease their level of dependence. Current research has already confirmed that muscle stimulations implemented into an FES neuroprosthesis is successful in holding the arm static at various joint positions (Wolf, 2017). Our simulations will expand on this research and allow for control of the shoulder and elbow as one functional unit to perform motion control while preserving the arms natural ability to choose different paths or muscle combinations to perform the same action instead of a fixed stimulation pattern. This research was completed as an initial step in developing a practical FES control strategy for functional reaching in individuals with high tetraplegia and presents an individualized equilibrium point controller capable of full-arm reaching movements for a static position from a set of muscle activations. Chapter II defines the underlying principles of motor control strategies of the Equilibrium Point Hypothesis and how it is utilized in this research. Chapter III defines the underlying principles of Gaussian Processes and Gaussian Process Regression and how they will be utilized in this research. Chapter IV identifies a virtual model and calculates muscle activations capable of holding static positions throughout a workspace. This leads to Chapter V in which muscle activations are used to quantify the size of the basin of attraction. Employing the data and information gathered from the previous Chapters, Chapter VI examines the capabilities of muscle activations within the basin of attraction to achieve full-arm reaching movements utilizing principles of the Equilibrium Point Hypothesis. Finally, Chapter VII will discuss the results and future aims of the research presented in this thesis.

CHAPTER II

EQUILIBRIUM POINT HYPOTHESIS

The Equilibrium Point Hypothesis has been a central theory in motor control since its introduction almost 30 years ago, and is the basis of the control strategy we are using to control the virtual arm (Feldman, 2009). The Equilibrium Point Hypothesis was originally developed for single joint arm movements, with more recent adaptations expanding into multi-joint arm movements. The hypothesis states that movements arise from shifts in the equilibrium position of the limb and that the equilibrium is a consequence of the interaction of reflex mechanisms, muscle properties, and external loads under the control of central neural commands (Feldman, 2009). The most common model within the Equilibrium Point Hypothesis, the λ model, defines movements of the limbs as being generated by the nervous system through a gradual transition of equilibrium points along a desired trajectory (Feldman, 1986). In this model, equilibrium points are defined as a state where a field has zero force, meaning opposing muscles are in a state of balance with each other, with λ corresponding to a unique configuration for a muscle, joint, or combination of joints. The λ model has been shown to account for a range of physiological data and research has verified its accuracy as a representation of how the human nervous system controls movement (Feldman, 1986). Utilizing the

Equilibrium Point Hypothesis as a basis of a control strategy allows us to examine its possibility as a simplified method of limb movement along a path.

The basis of the λ model originates from the suggestion that limb movements arise from the shifting of the equilibrium state of the motor system due to changes to neural control signals. Motor innervation to muscles arises from α motor neurons, which innervate the main body of the muscle, and from γ motor neurons, which contribute to α motor neuron excitation through reflexes. Electrochemical influences from the brain, in the presence of proprioceptive feedback to motor neurons, are transformed into changes in the threshold muscle lengths (λ) or joint angles at which the motor neurons begin recruiting. In response, muscle activations and forces vary in relation to the difference between the actual and the threshold muscle lengths and the rate of muscle length change. The change in activation results in joint torques and the resulting motion depends upon the muscle torques and external loads (Feldman, 1986). That is, muscle activation thresholds of various muscles shift between positions along a trajectory, simulating the movement between equilibrium points within the system. Thus, by shifting λ through changes to the central facilitation of motor neurons, the system can produce movement to a new equilibrium position (Sainburg, 2015). This allows control levels of the CNS to specify where, in spatial coordinates, muscles are activated to more accurately identify which muscle groups are required.

The Equilibrium Point Hypothesis has been used as a control strategy in several studies related to limb movement and robot control. Several studies performed focused on implementing an external force to the arm to verify if the arm returns to the initial equilibrium point once the force is removed. This is similar to the second aim of our research where an external force is used to move the arm out of place to estimate how far the arm can be moved before it will not return. One of the most common studies utilizing Equilibrium Point Hypothesis is the concept of muscle unloading, in which weights are hung on ropes attached to pulley systems attached by small electromagnetic locks and connected to a subject's arm (Archambault, 2005). The subject's arm initially establishes a specified position while counteracting a certain load torque to establish an initial target equilibrium point. Once the equilibrium point was established, the load was decreased, resulting in the motion of the forearm to another combination of the static torque and position (a new equilibrium point). The initial load was then restored and the subject established the same initial equilibrium point, and the trial was repeated with the same or a different randomly chosen final load. Thus, it was possible to record a set of equilibrium points resulting from unloading from the same initial equilibrium point. The tonic EMG activity of pre-loaded muscles was not the same for different equilibrium points as it monotonically decreased with the decreasing amount of the residual load and the displacement of the arm increased with the increasing amount of unloading (Archambault, 2005). In another study, a robotic arm was used to slowly displace a subject's hand from an origin and measured the restoring forces. The subject is then told to attempt to reach to a target while the robot measures the force the subject is generating to perform the movement. The magnitude and direction of movement-related forces agree with the hypothesis that movement is generated through a shift of the equilibrium position of the postural force field toward the target (Shadmehr, 1993). Several other studies focused on generating movement in a robotic arm outside of human control or a central nervous system by manipulating stiffness quantities to change equilibrium points

(Byeong-Sang, 2013; Gu, 2007). In these experiments, principles of the Equilibrium Point Hypothesis were used to potentially generate human arm-like motion by using actuators or damped springs in place of a nervous system to directly control the robotic arm. Control of the actuators or damped springs allowed for manipulation of the joint torques responsible for holding the equilibrium points to examine movement between these points without higher level control. These experiments proved that direct control of a robotic arm, in place of a central nervous system, utilizing the Equilibrium Point Hypothesis is possible.

The similarity of previous research studies to our hypothesis that full-arm reaching motions can be achieved through the transitioning of muscle activations between equilibrium points further solidifies our decision to use Equilibrium Point Hypothesis as a control strategy. In equilibrium point control, the general central equation of a control strategy is

$$\alpha = \left[l - \lambda + \mu \acute{l}\right]^{+} \tag{1}$$

where

$$[x]^{+} = \begin{cases} x, & if\ x > 0 \\ 0, & if\ x \leq 0 \end{cases}$$

where muscle activation, α, is proportional to the difference between the current muscle length, l, and the centrally specified threshold length, λ, as well as on the rate of muscle length change, $\acute{l}$, with μ specifying the dependence of the muscle's threshold length on velocity and provides damping due to proprioceptive feedback (Feldman, 1986). In this equation, the muscles act as a spring-damper with a dependence on velocity. We designed our central equation of a control strategy

$$M\alpha = \tau(q) \tag{2}$$

based on the underlying mechanics of our system where $\alpha \in R^{10x1}$ is a matrix of muscle activations, $M \in R^{5x10}$ is a matrix of linear mapping of activations of muscles to joint torques, and $\tau \in R^{5x1}$ are the joint torques required to maintain an arm configuration, q. The desired arm configuration, q, is chosen and the joint torques and muscle activations are developed to maintain the configuration. Generating these muscle activations by selecting a desired arm configuration is similar to generating muscle activations from the selected threshold length in Equation 1. In this respect, both equations identify equilibrium points from a selected set of initial conditions and corresponding activations, effectively moving between these points by only having to specifying either q or λ. However, since we are not receiving neural commands, as in Equation 1, our developed equation was based off a mechanical control strategy to achieve muscle activations, but still utilizing the underlying principles of the equilibrium point hypothesis control strategy. This control strategy develops muscle activations that are dependent on joint configuration and joint torques instead of muscle lengths and velocity as in Equation 1. Our strategy is used to identify muscle activations at static positions in which the arm would not be moving, in which velocity and muscle length would be constant. This means that maintaining the static position would be dependent on the configuration of the arm and the joint torques required to hold the arm in place instead of muscle length or velocity. Although the arm is moved using an external force in the basin of attraction simulations, which would implement a muscle length change and velocity into the model, the muscle activations aim to evaluate if configuration and joint torque dependency can overcome these factors. Our control strategy model allows for M and τ to be calculated from Gaussian Process Regression for a given arm configuration to determine the corresponding muscle activations.

There has been a great deal of controversy regarding the Equilibrium Point Hypothesis and a desire to reject the hypothesis entirely due to several unresolved limitations. The current limitations of the Equilibrium Point Hypothesis include violations in predictions of the principle that a given end position can be reached by many potential means in an open system, whether muscle resistance to displacement is adequate to support motor control, and a limited description of how the complexity of spinal circuitry might be integrated to yield a unique and stable equilibrium position for a given motor neuron threshold (Feldman, 2005). However, despite these limitations, the Equilibrium Point Hypothesis is still widely used today because it offers a unique solution to issues that other methods, such as the force control hypothesis and dual-strategy hypothesis, have not been able to overcome. These issues include resolving the posture-movement paradox – when posture-stabilizing mechanisms resist deviations produced by external forces but not those produced by voluntary movements - and including the co-activation of opposing muscle groups (Feldman, 2005). The force control and dual-strategy hypotheses neglect these factors, leaving them physiologically infeasible (Feldman, 2003; Monohar, 1998). The Equilibrium Point Hypothesis continually adapts to new information and technologies, further strengthening its underlying principles and making it a strong hypothesis to utilize despite its limitations.

Fundamentally, the Equilibrium Point Hypothesis suggests that simple, direct control signals from the brain may underlie smooth joint movement of a system along a trajectory from a starting position to an ending position using equilibrium points. Using the basic principles of the Equilibrium Point Hypothesis, we calculated muscle activations at specified equilibrium points in a reachable space to examine limb movement between these equilibrium positions. This was accomplished by examining the basin of attraction around several joint positions in the workspace using activations of various muscle groups and external forces (Chapter V). If a joint is in equilibrium, any deviation caused by external sources will generate muscle forces to bring the joint back to its equilibrium. In this case, the basin of attraction - a set of points from which a system approaches a stable position – exists around the equilibrium point for a set of initial joint position conditions. Consequently, if a basin of attraction exists for joint positions and muscle activations throughout the workspace, we can use this data to examine the feasibility of an equilibrium point control strategy along a trajectory utilizing the principles of the Equilibrium Point Hypothesis (Chapter VI).

CHAPTER III

GAUSSIAN PROCESS REGRESSION

Gaussian Processes (GPs) and Gaussian Process Regression (GPR) are statistical modeling methods that were critical in this research for their utilization in estimating joint torques required to hold any joint position in the workspace. In general, statistical models are mathematically-formalized models, embodying a set of assumptions concerning the generation of sample data from a larger population, to approximate a real system and, optionally, to estimate probabilistic future behavior from this approximation (Rasmussen, 2006). In this research, joint torques required to hold static positions will be accumulated to utilize GPR to determine joint torques for any joint configurations that correspond to equilibrium positions.

One of the most common methods of statistical modeling is a GP, a collection of random variables, any finite number of which have a joint Gaussian distribution. Figure 1 below shows a distribution of functions drawn from a Gaussian Process. Before any data is observed for a GP, a prior probability distribution (prior) must be identified. A GP defines a prior over functions by implementing constraints on the system, such as limiting the domain, specifying the mean, and describing the smoothness to produce ideal functions over the prior distributions. The covariance function specifies the smoothness of the GP by relating the outputs for two different inputs and ensuring that values that are close together in the input space will produce comparative output values and, along with the mean function, completely defines a GP (Rasmussen, 2006). The generalized equation for a squared exponential covariance function can be seen in Equation 3 below

$$k(x, x') = exp\left(\frac{-(x-x')^2}{l}\right) \tag{3}$$

where $k(x, x')$ is the covariance function that describes unity between variables whose corresponding inputs are very close, and decreases as their distance in the input space decreases, x and $x'$are two points in the input space, and l is the characteristic length-scale.

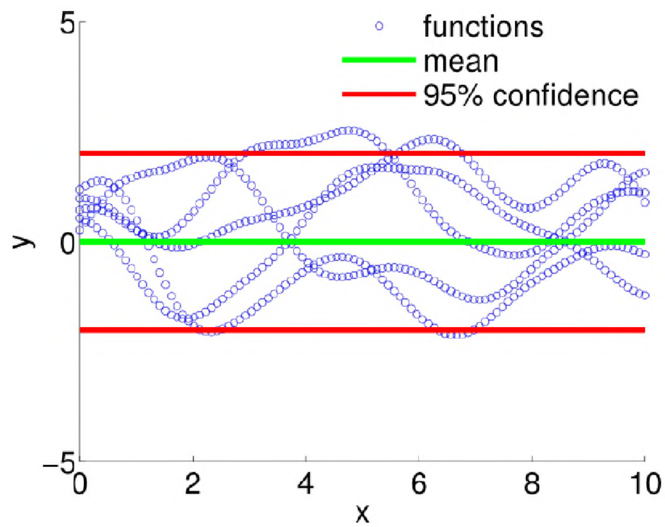

Figure 1 Example Gaussian Process A distribution of functions drawn from a Gaussian Process

Once the prior has been defined, it can be converted into a posterior over functions using observed data. Remaining points of the function are estimated by generating a probability distribution that assumes that the observed and estimated data are jointly Gaussian. After implementing the observed data points into the prior, the posterior becomes the joint probability of outcome values of both observed and unobserved values, generating a distribution over all possible functions that are consistent with the observed data. This reduces the set of all possible functions in the prior to only the functions that connect the observed data points in the posterior, as seen in Figure 2 below. Generating a posterior ensures that observed data and test data fall within the mean and covariance parameters of the GP to accurately quantify the distribution.

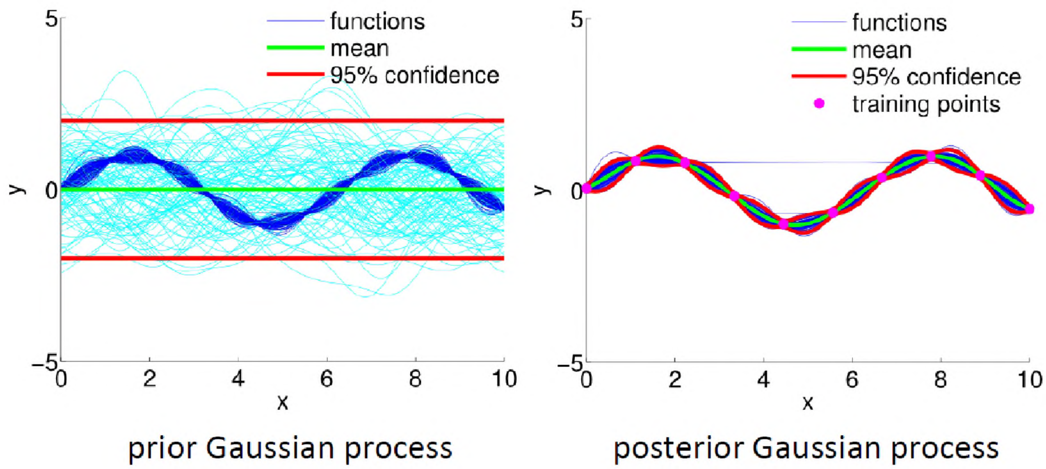

Figure 2 Example Prior and Posterior Gaussian Process In a prior Gaussian Process, a probability distribution is expressed about an uncertain quantity before observations are taken into account. Once observations are identified, a posterior can narrow down the probability distribution to only functions that include observation points and that follow the mean and covariance parameters

Once a GP is established, it can be used as a model for GPR to predict outputs for inputs not in the observed dataset by assuming the training and test data are jointly Gaussian. GPR is used to compare observed training data in a posterior to predict test output values from a desired test input. Training data is the data accumulated during previous trials of the simulation that are used for learning and fitting of the covariance function and hyperparameters. Test data is a dataset that is independent of the training data, but follows the same probability distribution so that output for the test data can therefore be interpreted. In this research, the training and test data consists of an input of joint angles that correspond to a joint configuration and an output of joint torques required to hold the arm in the desired configuration. GPR was used to estimate joint torques and muscle activations necessary to hold any desired input position from observed joint torques and activated muscle groups in various positions throughout the workspace. The joint distribution of the observed target values and the function values at the test locations under the prior that defines the mean and covariance under the prior is defined in Equation 4. The key predictive Equations 5 and 6 define the predictive distribution of the output given a new input and training data

$$\begin{bmatrix} y \\ f_* \end{bmatrix} \sim N\left(0, \begin{bmatrix} K(X,X) + \sigma_n^2 I & K(X,X_*) \\ K(X_*,X) & K(X_*,X_*) \end{bmatrix}\right) \tag{4}$$

$$\bar{f}_* \triangleq \mathrm{E}[f_* \mid X, \mathrm{y}, X_*] = K(X_*,X)[K(X,X) + \sigma_n^2 I]^{-1} y \tag{5}$$

$$\mathrm{cov}(f_*) = K(X_*,X_*) - K(X_*,X)[K(X,X) + \sigma_n^2 I]^{-1} K(X,X_*) \tag{6}$$

where X are the training inputs, X_* are the test inputs, $\bar{f}_*$ is the GP posterior mean, f_* is the GP posterior prediction, σ_n^2 is noise variance, $K(X,X_*)$ is a covariance matrix of training inputs and test inputs, and I is an identity matrix (Rasmussen, 2006). These equations are used to define the predictive distribution of output given new input and training data. In this research, several joint configurations were examined as training data and the torques required to hold configurations static were found. GPR was then used with the training data to calculate torques for a desired joint configuration. An optimization problem was then used on the output from GPR to calculate the muscle activations required to maintain any joint position in the workspace (Chapter IV).

In addition to GPR, there are numerous methods of statistical modeling that can potentially be used for predictive learning including: linear regression, Kernel Ridge Regression, Locally Weighted Projection Regression, and neural networks. Linear regression is a linear approach for modeling the relationship between a scalar dependent variable and one, or multiple, independent variables. It works similar to GPR, but the output is a linear combination of fixed linear regression basis functions that use parameters that are adjusted to fit the model to the data, often using the least squares approach. However, linear regression outputs optimal results when relationships between the fixed basis functions and dependent variables are almost linear, which tends to lead to over fitting of data if too many basis functions are chosen or too big of an error if not enough basin functions are chosen (Murphy, 2012).

Kernel Ridge Regression (KRR) is a method for performing nonparametric regression – regression analysis in which the predictor is constructed according to information derived from the data, not from a predetermined form such as linear regression - similar to GPR (Murphy, 2012). However, unlike GPR, KRR is able to learn a linear function in the kernel space, based on the mean-squared error loss with ridge regularization, which corresponds to a non-linear function in the original space, as seen below in Equation 7.

$$f(x) = y'(K + \lambda I)^{-1}k \tag{7}$$

where *f()* denotes an arbitrary function, K denotes the kernel, I is an identity matrix of the relevant dimension, λ is the regularization parameter that adds rank to K, and k is the vector of inner products between the data and the new point, x. However, GPR can define hyperparameters – parameters of the prior distribution such as length-scale, signal, and noise - based on gradient-ascent on the marginal likelihood function while KRR needs to perform a grid search on a cross validated loss function. The marginal likelihood – the likelihood of observing the data given the hyperparameters marginalized over the distribution of functions defined by the hyperparameters - is equivalent to the integral of the likelihood times the prior and can be seen in Equation 8 below.

$$p(y|X) = \int p(y|f, X)p(f|X)df \quad (8)$$

Choosing hyperparameters allows GPR to learn a generative, probabilistic model of the target function capable of providing meaningful confidence intervals and posterior samples along with predictions, while KRR is limited to only providing predictions.

Locally Weighted Projection Regression (LWPR) achieves nonlinear function approximation by using locally linear models, spanned by a few univariate regressions in selected directions in input space, and cycles through datasets multiple times. However, LWPR is inefficient at computing non-local points and requires large sample sizes (greater than 2,000); otherwise, samples need to be presented multiple times in random order (Murphy, 2012). GPR is more successful and practical at handling smaller sample sizes as accurately as LWPR without repeatedly cycling through a dataset. In this research, we are limited to a small sample size due to the limitations in human experiments that can be performed as there is a limited amount of time to collect training data and we are constrained to a relatively small workspace when working with human subjects.

Finally, neural networks are commonly used because of their iterative learning process and are comprised of a set of input values, associated weights, and a function that sums the weights and maps the results to an output. A neural network consists of nodes in multiple layers, with the connections between nodes of adjacent layers having weights associated with them. Initially, weights are randomly assigned and, for every input in the training dataset, the neural network is activated and its output is observed. This output is compared with the desired output that is already known, and the error is propagated back to the previous layer. The error is noted and the weights are adjusted accordingly, with the entire process repeating until the output error is below a predetermined threshold (Nielson, 2015). This creates a learned neural network which can then work with new inputs. However, neural networks are difficult to train, depend crucially on initial parameters, and are not probabilistic.

Despite its advantages over other methods, one of the largest drawbacks of GPR is that it becomes computationally expensive for larger dataset (greater than 1,000). Due to our small sample size, the ability of GPR to compute confidence intervals and marginal likelihoods, and the ability to automatically choose the model, GPR was chosen as the most appropriate statistical modeling method for our research.

CHAPTER IV

MAINTAINING HOLDING FOR STATIC POSITIONS

Generating the ability to maintain holding for static positions was a necessary first step in determining if equilibrium point control of full arm reaching motions was feasible. To maintain a static position, we must identify the activation requirements of separate muscle groups to sustain a configuration while overcoming gravitational forces. Previous research has already shown that when stimulated with an FES neuroprosthesis, an individual with high-level tetraplegia was capable of maintaining a desired static position from calculated muscle stimulations (Wolf, 2017). However, static holding is the extent of this research and full movements were not examined. To expand upon the results found in Wolf, a computer-simulated virtual model of a human arm was used to implement muscle activations on static positions to examine the feasibility of full-arm reaching movements.

We generated our own model from the virtual arm to allow us to determine the arm's response to muscle activation and to simulate real-world conditions in which a ground truth model would not exist. In Section 4.1, the parameters of the virtual arm were identified and the target muscles and joint angles were chosen. In Section 4.2, training data throughout the workspace was accumulated using external forces and internal activations of the virtual arm to identify a model. Section 4.3 uses the model to develop a controller capable of calculating muscle activations necessary to hold the arm in any desired static position in the virtual workspace. Holding the arm in position allowed the virtual model to output the joint angles and forces at the end of the forearm required to maintain that position while fully activating a target muscle group. In Section 4.4, the accuracy of the controller was evaluated for twenty separate static positions in the workspace. Sections 4.5 and 4.6 examine the results and discussion identified in this Chapter. Determining if static holding is feasible in a virtual arm will be able to identify how separate muscle groups work together to maintain a variety of joint configurations which can be further examined for the existence of a basin of attraction. The objective of this chapter was to verify if identified muscle activations were capable of maintaining static positions.

4.1 Simulation Setup

Simulations were performed on a virtual human arm model developed with Matlab coding and visually represented with the OpenSim Dynamic Arm Simulator (DAS) (Chadwick, 2014). Inputs to the Matlab code controlled external support forces and internal simulations within the DAS capable of producing full-arm motions. External support forces were applied at the end of the forearm and were used to initially move the arm into desired positions while internal stimulations were used to simulate the activation of specified muscle groups.

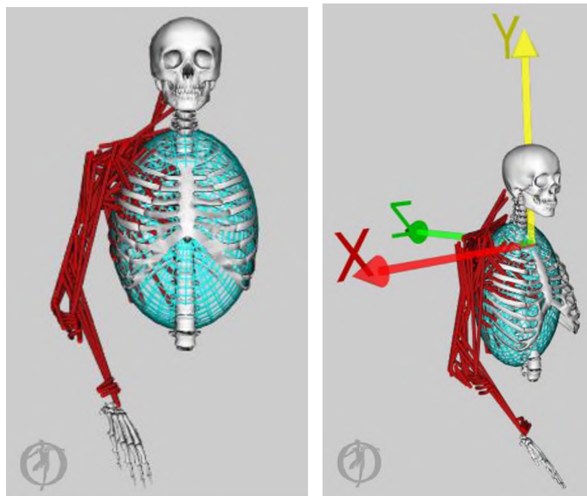

Figure 3 Dynamic Arm Simulator A virtual model of a human right arm and the corresponding OpenSim coordinate system

Figure 3 above shows the complete DAS, which is comprised of articulated joints, skeletal structure, 11 degrees of freedom, and 138 muscle fibers comprising 28 separate muscle groups of a human right arm of weight and length determined from cadaver studies (Chadwick, 2014). The muscle fibers are individually activated to simulate muscle stimulation, with several muscle fibers constituting one muscle group. When a particular muscle group is activated, the entire group of related muscle fibers is stimulated to simulate full activation of that muscle group.

First, of the 11 degrees of freedom within the DAS, only 5 were examined in this research to define joint angles. The 5 degrees of freedom examined were shoulder abduction, shoulder rotation, shoulder flexion, elbow rotation, and elbow flexion. The chosen degrees of freedom defined the configuration of the shoulder and elbow to designate the position of the wrist in the workspace. The other 6 degrees of freedom were not examined as they were the degrees of freedom of the thorax and had limited to no significance on the shoulder or elbow. Second, from the 28 separate muscle groups within DAS, 10 were examined in this research as seen in Table I, chosen for having a strong influence on full-arm reaching movements. These muscle groups were shown to have the strongest effect on shoulder abduction, shoulder rotation, shoulder flexion, elbow rotation, and elbow flexion of the muscles during full-arm movements. The remaining 18 muscle groups were not examined as they dealt with the movement of anatomical groups we were not examining in this research such as the scapula and sternum. Lastly, the position of the wrist was defined in relation to the top of the sternum on the thorax on a 3D coordinate system, Figure 3. The X-coordinate defined the horizontal left and right movements of the end of the forearm of the DAS, the Y-coordinate defined the vertical movements of the end of the forearm of the DAS, and the Z-coordinate defined the horizontal forward and backward movements of the end of the forearm of the DAS. The chosen DAS degrees of freedom and related joint torques were used to define the configuration of the arm with respect to the shoulder and elbow.

Target Muscle Groups and Their Functions	
Muscle	**Function**
Serratus Anterior	Anteversion of arm, aids in arm elevation
Delta Clavicle	Flexes and medially rotates arm
Biceps	Forearm supination and elbow flexion
Rhomboids	Scapula retraction
Infraspinatus	Shoulder rotation
Supraspinatus	Abduction of arm at shoulder joint
Pectoralis Major	Flexion and extension of shoulder, medially rotates arm at shoulder
Latissimus Dorsi	Extension, adduction, and transverse extension of arm at shoulder
Brachialis	Arm flexion at elbow
Triceps	Retroversion and adduction of arm

Table I Muscle Groups and Functions

4.2 Model Identification

To simulate real-world conditions in which a ground truth model would not exist, we identified our own model from DAS to allow us to examine the arm's response to the activation of specific muscle groups. A two-part model was developed consisting of GPR models of inverse statics (the mapping from configuration to joint torques) and muscle torque production (the mapping from configuration and activation to the torques produced), seen below in Figure 4, necessary for calculating joint torques and muscle activations for any position in the workspace. In previous experiments, model identification has been used on a human subject to obtain muscle activations necessary to hold a static position. One experiment in particular used a robotic arm with a three-dimensional force sensor at its end-effector to hold the arm of an individual with high-level tetraplegia in place and output forces at the end of the forearm (Wolf, 2017). To recreate this experiment in our simulation, an external force was used to mimic the actions of the robotic arm by holding the virtual arm in place to gather data and generate the forces at the end of the virtual forearm required to maintain its position.

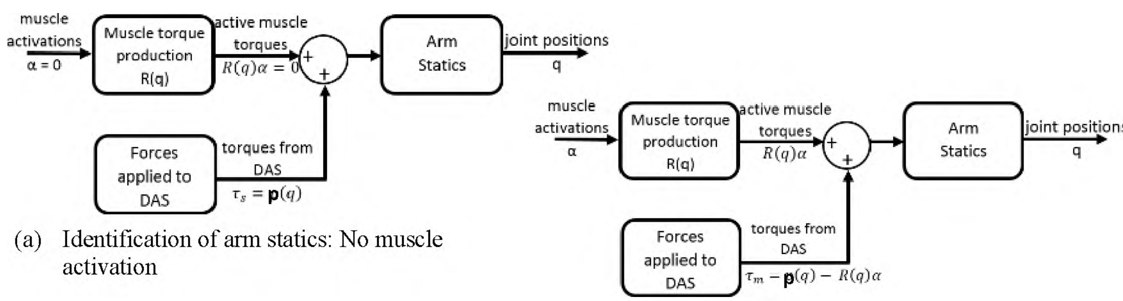

(a) Identification of arm statics: No muscle activation

(b) Identification of muscle torque production: Activation of one muscle group

Figure 4 Identification of Arm Statics and Muscle Torque Production The torques from DAS, τ, are the shoulder and elbow torques which would produce the same static position as the force applied by the model during a trial. For a given joint configuration, q, when no muscle groups are activated (a), the model torques are equal to the torques, **p**(q), required to hold the arm in the configuration. With one muscle group activated at 100%, the model torques are equal to the difference between **p**(q) and the torques produced by the muscles (b). For each trial, we chose the muscle group activation, computed the model torques, and used the identification technique to determine the arm statics and muscle torque production blocks.

To gather data for the model identification, an external force held the virtual arm at a position within the workspace. To gather joint torques and muscle activations for a desired joint position, the DAS utilized a combination of external and internal forces to achieve and maintain a desired joint position from an initial set of Cartesian coordinates. Two sets of external force proportional-derivative (PD) controller gains were used to manipulate the arm separate of muscle influence. A PD controller with an initial set of gains was used to move the arm to a desired position without any muscle activations while a second set of PD controller gains was used to keep the arm held in the desired position while muscles were activated. The second PD controller was initially hand-tuned by manipulating the proportional and derivative gains to keep the arm static when muscle activations were implemented. The initial PD controller gains moved the arm to a given Cartesian point in the reachable space, corresponding to a desired position of the wrist, for several seconds and was then removed. The second PD controller gains were then implemented to hold the arm in the desired position for another several seconds while a single muscle group was activated to 100%. This was repeated for all ten muscle groups at twenty separate positions throughout the workspace, seen below in Figure 5, chosen to reach as many distinct points in the workspace as possible to provide a wide sampling of the workspace while still maintaining a small dataset. We limited the positions examined to 20, to mimic the amount of data that would reasonably be achieved during a real human experiment but still reach a wide variety of locations in the workspace. Holding the arm in position allowed the DAS to output the joint angles and forces at the end of the forearm required to maintain that position while fully stimulating a target muscle group.

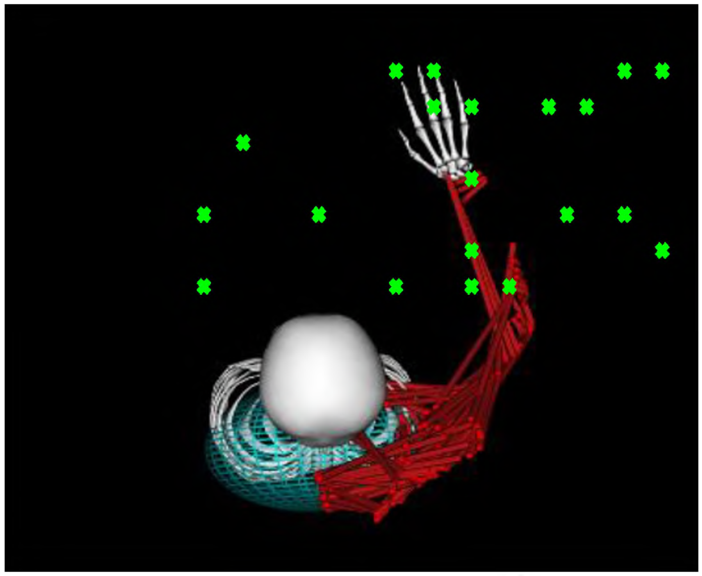

Figure 5 Training Positions Pictured is an overhead view of the virtual arm. Each green mark represents a target joint position for which we gathered data to identify our model. Positions were chosen to reach a wide variety of training points in the workspace

The accumulated data of joint angles and forces at the end of the forearm had to be converted to joint torques to identify components of the model. The kinematic Jacobian of the arm at the wrist was computed for each joint position and then used to determine the joint torques about the shoulder and elbow that would sustain the specific static position, as seen in Equation 9 below

$$\tau = J^T F \tag{9}$$

where $\tau \in R^5$ are the joint torques about each degree of freedom for the static configuration, J^T is the transpose of the Jacobian matrix, and F is the vector of forces at the end of the forearm required to hold the virtual arm static.

Calculating joint torques from the combination of joint angles and forces at the end of the forearm was necessary in finding the arm statics and muscle torque production to fully identify the two part model. To determine arm statics, the virtual arm was held in the joint position with the PD controller without any muscles activated (Figure 4(a)).

That is, the activation of muscles, α, was equivalent to zero. As such, $\mathbf{p}$ was defined as the vector of torques necessary to hold the arm in the static configuration while no muscles were activated, determined by the joint angles of the shoulder and elbow, where the joint angles are defined in (Wu, 2005). To determine the torque contribution of a single muscle group, the arm was moved to a target position, and a muscle group was 100% activated while being held in place by the second PD controller gains. The DAS then outputs the joint angles of the position and forces at the end of the forearm produced by that specific muscle group (Figure 4(b)). The joint torques for both arm statics and muscle torque production were determined from the ending forces and Jacobian, a function of the joint angles, as seen in Equation 9 above. The joint torque calculations with muscle torque production included both the passive torque and active muscle torque contributions as seen below

$$\tau_m = \mathbf{p} - R\alpha \tag{10}$$

where $R \in R^{5x10}$ is the linear mapping of activations of muscles to joint torques, $\mathbf{p}$ are the passive joint torques found when no muscles are activated, α is a muscle activation vector of all zeros except for a value of one for the muscle group being activated, and τ_m is the total torque contribution when a muscle group is activated. The elements of R were found by manipulating Equation 10 and subtracting the passive torques from the model torques as seen below

$$R\alpha = \mathbf{p} - \tau_m \tag{11}$$

where the element of α that corresponds to the activated muscle group is equal to one and R is the linear mapping of activations of muscles to joint torques without a passive influence. For the examined joint positions, each row of R corresponds to the torque about a specific degree of freedom, and each column represents the torque produced by the 100% activation of a target muscle group.

To train a GPR model capable of determining $\mathbf{p}(q)$ and $R(q)$ for any joint configuration, q, within the workspace, arm statics and muscle torque production values, $\mathbf{p}$ and R, were calculated for the 20 target positions to estimate mean and covariance functions. Using Equations 5 and 6 from Chapter III and repeated below, we can implement the $\mathbf{p}$ and R values into the predictive equations for GPR.

$$\bar{f}_* \triangleq \mathrm{E}[f_* | X, \mathrm{y}, X_*] = K(X_*, X)[K(X, X) + \sigma_n^2 I]^{-1} y \tag{5}$$

$$\mathrm{cov}(f_*) = K(X_*, X_*) - K(X_*, X)[K(X, X) + \sigma_n^2 I]^{-1} K(X, X_*) \tag{6}$$

Using Equation 5 with our data, we can find the GP posterior mean, $\bar{f}_*$, where X is the training data of joint angles for arm configurations we examined, X_* is the test data of joint angles for the joint position desired, y is the vector of our arm static data $\mathbf{p}$, $K(X, X)$ is the covariance matrix between points of the training data with added noise variance, σ_n^2, and $K(X_*, X)$ is the covariance matrix between points of similar training data and test data. Utilizing Equation 6 with our data, we can find the GP posterior covariance, $\mathrm{cov}(f_*)$, where $K(X_*, X_*)$ is the covariance matrix between points of the test data, I is an identity matrix, and $K(X, X_*)$ is the covariance matrix between training and test data. The combination of Equations 5 and 6 predict the torques given the training data and new joint angles. These equations are repeated for all 5 DOFs that constitute the joint position. Therefore, using the identity equations for GPR, the accumulated $\mathbf{p}$ and R training data can be used to estimate $\mathbf{p}(q_*)$ and $R(q_*)$ values for a set of desired test inputs.

4.3 Controller

Using the model identified in the previous section, our controller applies open-loop simulation inputs to GPR models necessary to hold a desired set of joint angles. An overview of the controller comprised of the two GPR models can be seen below in Figure 6. The input to the controller is a set of joint angles, $q_* \in R^5$, corresponding to a desired joint position in the workspace. The elements of the joint position are comprised of the shoulder elevation plane, shoulder elevation, shoulder rotation, elbow flexion, and elbow pronation. Given the joint angles of a desired joint position, the controller uses GPR to first generate the static joint torques required to hold the desired position. The controller process along with GPR is necessary in determining the activations of the chosen muscle groups required to achieve the desired joint position.

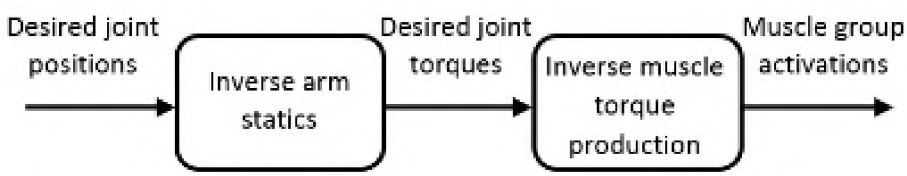

Figure 6 Controller Block Diagram

Utilization of a GPR model with the developed controller calculated arm statics and muscle torque production data required to hold a desired position. GPs and GPR are described in detail above in Chapter III. The first block of the controller used the GPR model of arm statics to calculate the desired joint torques, $\mathbf{p}(q_*)$, necessary to hold the desired configuration. The second block of the controller used the GPR model of muscle torque production to identify the elements of the mapping from muscle group activations to joint torques, $R(q_*)$.

To determine the required output of each muscle group to maintain the desired joint position, accumulated training data of joint torques for various joint configurations was used to calculate desired muscle activations. Once the desired joint torques, $\mathbf{p}(q_*)$, and mapping, $R(q_*)$, were identified, the muscle activations, α, required to hold q_* could be calculated by solving $R(q_*)\alpha = \mathbf{p}(q_*)$. However, since there were more muscle groups than there were degrees of freedom, $R(q_*)$ was not square and the equation had to be solved via optimization. To achieve a feasible set of activations, we minimized the sum of squares of muscle activations and optimization in the form of

$$\begin{aligned} &\underset{\alpha}{\text{minimize:}} \ \ \|\alpha\|_2^2 \\ &\text{subject to: } R(q_*)\alpha = \mathbf{p}(q_*) \\ &\qquad\qquad\quad \alpha_i \in [0,1] \quad \forall \in \{1,2,\ldots,10\} \end{aligned} \tag{12}$$

was used and then solved via the Matlab quadratic programming function 'quadprog'. A set of muscle activations, corresponding to each muscle group, was returned if the quadratic program is feasible and a flag was returned if no solution could be found. With α,$\mathbf{p}(q_*)$, and $R(q_*)$ identified, the GPR model with the developed controller had successfully identified all information necessary to examine if a static position could be maintained.

4.4 Static Hold Simulations

To assess the controller's ability to hold static positions, we quantified its accuracy at 20 joint positions in the workspace that were different than the positions used to train the model. Targets were selected at various locations throughout the DAS workspace to simulate a wide range of reaching motions close to and far away from the front, left, and right side of the body, as well as at locations at, above, and below the middle of the chest, as seen in Figure 7 below. The controller from Figure 6 was then used to determine the muscle activations for the desired target position. To move the arm initially into the target position, the initial PD controller gains were used to position the arm while no muscles were activated to allow the beginning of every simulation to be identical. Once the arm was at the target position, muscle activations were applied while the second set of PD controller gains were used to hold the arm stationary. After holding for one second, the PD controller was turned off, allowing the arm to move freely for 5 seconds exclusively using the activation of the muscles. The joint angles and coordinates of the wrist were output from the DAS and recorded. An ideal controller would result in a stationary joint position for the entire trial, while a less than perfect model would result in the arm moving away from the target position.

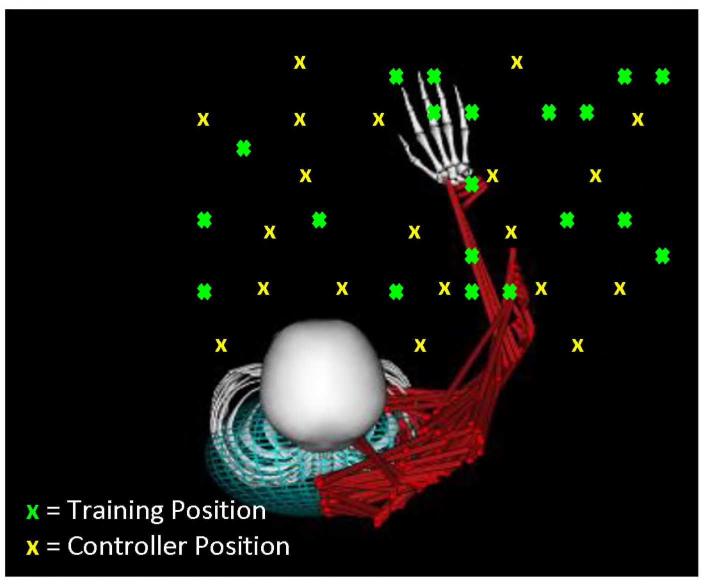

Figure 7 Controller Positions Twenty positions, separate from the training positions, were used to assess the controller's ability to identify muscle activations to hold static positions at varying distances away from the training positions. Positions were chosen at varying distances away from training positions to examine the capability of the controller to reach additional positions.

4.5 Results

A controller capable of determining joint torques and muscle activations to successfully hold twenty desired joint positions was developed. Using the accumulated data of the training positions and the identified model, the controller was able to calculate desired muscle activations, ranging from 0 to 1 (corresponding to 0% to 100% activation), required from each target muscle group to achieve a set of desired joint angles, as seen in Figure 9 below. Comparing the distances between the final joint position obtained and the target joint position for the static holding simulations, an averaged Euclidean distance of 1.1 $\pm$ 0.13 cm standard deviation for all 20 joint positions was obtained. The distribution of all final distances from the target can be seen in the histogram in Figure 8 below, with half of the final distances from the designated target falling around roughly 1.1 cm. The success of the controller to maintain desired static positions implies that our process of accumulating data and identifying a model was effective in the development of the controller and that the underlying statics of the arm can be identified and used to our advantage.

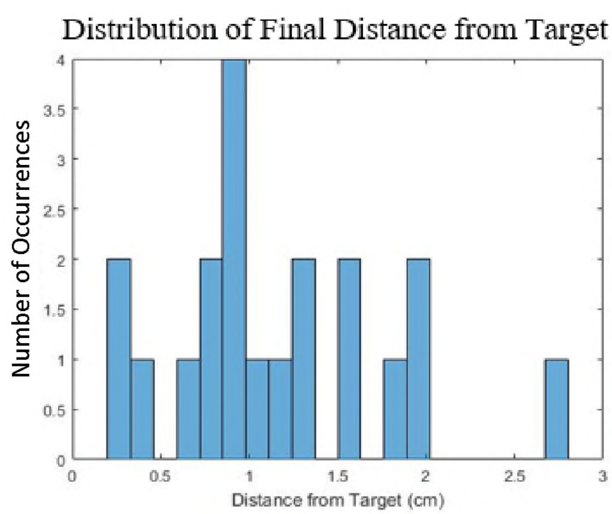

Figure 8 Histogram Frequency of ending distances of twenty target positions from the original static position

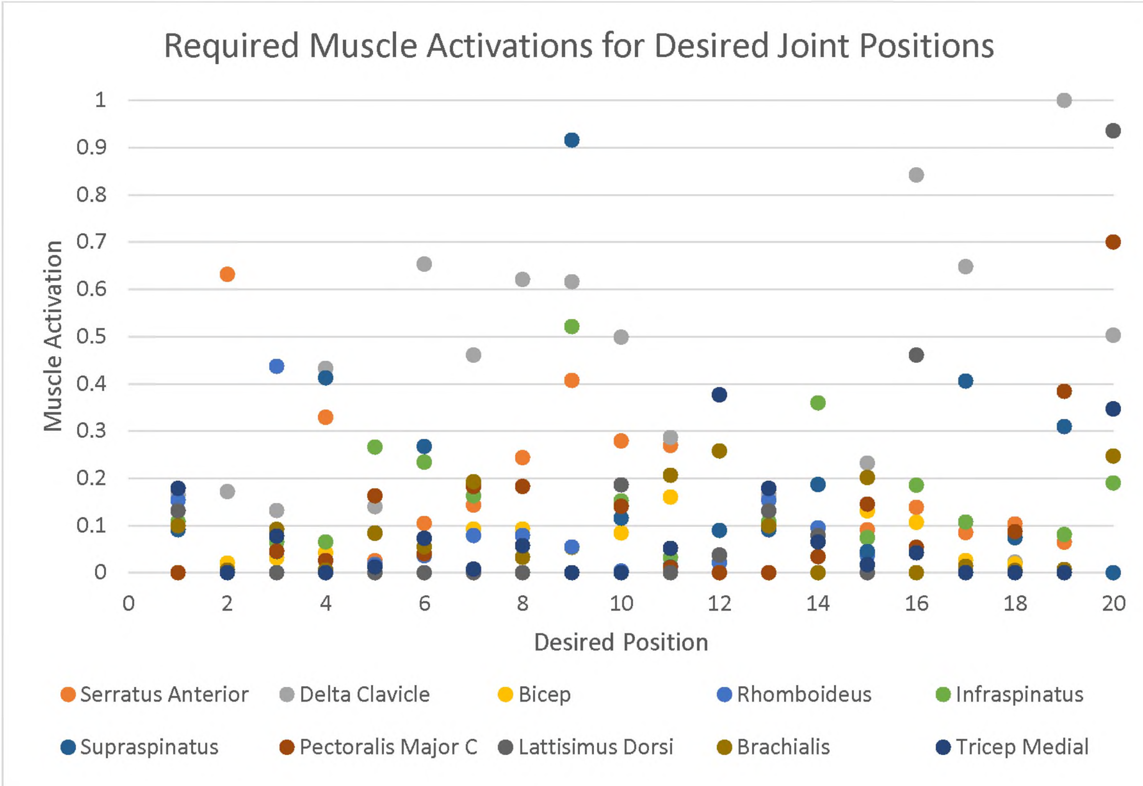

Figure 9 Controller Muscle Activations Muscle activations generated from the controller GPR models required to hold each of the controller positions throughout the workspace. It is apparent that, depending on the position in the workspace, varying activations of muscles are needed, stressing the importance of developing a controller

4.6 Discussion

Static holding simulations were used to determine if muscle activations capable of maintaining a desired joint position could be generated from a model and a controller. The capability of generated muscle activations to successfully sustain a static position without external assistance within 1.1 ± 0.13 cm of the target position demonstrated that static holding is feasible and reasonably precise. The static holding simulations focused on a model composed of only 20 joint positions and a larger sample size may have resulted in a more accurate controller. Current human research studies have demonstrated that, with the aid of a robotic arm, muscle stimulations for a specified position can be generated from a controller using a human subject with high-level tetraplegia as the model (Wolf, 2017). Calculated muscle stimulations were then implemented into an implanted FES neuroprosthesis to provide electrical stimulation to various arm muscles in the human subject and can maintain the desired position. Using this knowledge, the controller we developed can be expanded for implementation into human trials by adding a third controller block to invert recruitment curves to convert muscle activations obtained by the second block of the controller to muscle stimulation inputs. Stimulation inputs are necessary for implementation into an FES neuroprosthesis implant as they are the electrical amplitude equivalents of the muscle activations required to recreate movement in a human arm. Future research will add this third controller block to attempt to recreate simulations into human high-level tetraplegia subjects. This thesis focused on least squares muscle activations to reduce potential muscle fatigue when implementing into human subjects. The ability to identify muscle activations capable of static holding allows for further investigation into the development of transitional movement between these points.

CHAPTER V

BASIN OF ATTRACTION SIMULATIONS

To be able to move successfully between equilibrium points, we first need to identify static points as equilibrium points and the size of the basin of attraction to detect feasible moveable distances between potential equilibrium points. One important aspect of the Equilibrium Point Hypothesis is that it resolves the posture-movement paradox, the idea that posture-stabilizing mechanisms resist deviations produced by external forces but not those produced by voluntary movements (Feldman, 2009). That is, equilibrium positions of a system will resist externally implemented deviations to maintain its stable condition at the given equilibrium point. Utilizing the principles of the Equilibrium Point Hypothesis, equilibrium points – points where a field has zero force, meaning opposing muscles are in a state of balance with each other - of a system can be identified by having a nonzero basin of attraction size, as within this area the initial conditions are capable of overcoming the external forces imposed on the arm. The area around the equilibrium position in which the arm returns to the initial state is classified as the basin of attraction, a set of initial conditions from which a dynamical system spontaneously moves to a particular state. The previous chapter identified initial conditions for several static positions, but was unable to completely identify them as potential equilibrium points.

The ability of muscle activations to maintain a static position implies that the combination of muscle lengths and force values potentially generates an equilibrium point. Examining the basin of attraction would allow us to completely validate static positions as equilibrium points and identify the size of the basin of attraction that would permit the initial conditions to move back to its stable state. In Section 5.1, a trial simulation was performed to determine the appropriate sample size required for further simulations. This leads into Section 5.2 where, using the data from the static holding simulations and sample size calculations, we examined how the arm responded when an external disturbance moved the arm out of place to estimate the existence and size of the basin of attraction for various static positions. To achieve this, the arm was moved using the respective PD controller gains to the twenty joint positions from the static holding simulations. An external force was used to move the arm away from the potential equilibrium point for 15 seconds and then removed. This allowed us to examine the basin of attraction size and if internal muscle activations were able to overcome the deviations imposed by an external force to identify the position as an equilibrium point, which is further discussed in Sections 5.3 and 5.4.

5.1 Sample Size Determination

To perform enough simulations so that there is enough statistical power to detect differences between various basin of attraction sizes and differences between achieved and target ending positions, a sample simulation was run on a static joint position held in place with muscle activations. A joint position in the workspace was chosen from the group of twenty simulation points and the muscle activations to hold the position static were generated from the developed GPR model controller. The arm was initially moved into the joint position without muscle activation. Muscle activations were then implemented to hold the arm in the static position, similar to the static arm holding simulations above. Once the arm was held in place with the muscle activations, an external force was introduced for 5 seconds to force the arm to 15 different locations at varying distanced spheres around the static joint position. The external force was removed and the arm was given an additional 5 seconds to move freely exclusively using the muscle activations. The static arm position, ending position obtained, and distance between the two was recorded for all 15 arm movements. Equation 13 below was used to estimate an appropriate sample size utilizing the information gathered from the sample simulation,

$$n = \left(\frac{Z\sigma}{E}\right)^2 \tag{13}$$

where n is the sample size, Z is the value from the table of probabilities for a 95% confidence interval, σ is the standard deviation of the sample simulation in final ending distance between the achieved and target ending positions (σ = 0.827), and E is the margin of error we would like to be able to detect (E = 0.457 cm) (Sullivan, 2017). From the sample simulation data, it was determined that a sample size of 13 samples per basin size can determine changes in E 90% of the time for a 95% confidence interval.

5.2 Simulation Review

To determine the size of the basin of attraction and define static positions as equilibrium points, external forces were implemented onto the joint positions from the static holding simulations. For each static joint position chosen, muscle activations were generated from the developed controller. To allow every simulation to begin alike and reduce potential errors, an initial set of PD controller gains was used to initially move the arm into the static position while no muscles were activated. The PD controller gains were removed and the specific muscle activations for the static position were applied to the arm to hold the static position for 5 seconds. Once the arm had been held in place with the muscle activations, an external force was implemented for another 5 seconds to introduce a disturbance to the arm being held static. Implementation of the disturbance was performed by forcing the hand to 13 evenly spaced positions, determined from the sample size calculation, for each 5 cm, 10 cm, 15 cm, and 20 cm distance sphere around the static joint position. After 5 seconds, the external force was removed and the arm was allowed to move freely exclusively using the muscle activations. If muscle activations returned the arm near to the static joint position, the arm was determined to still be within the basin of attraction. The static position was determined to be an equilibrium point if the arm was moved to the 5 cm sphere and returned to the initial position within the sphere. The final estimated size of the basin of attraction was identified as the largest sphere size reached in which the arm still returned back towards the initial position and within the 5 cm sphere size. The chosen static position, ending position obtained, and distance between the two was recorded for each sphere, with the simulation being repeated for all 20 static joint positions. The averaged Euclidean distance between the static position and ending position obtained was used to determine the accuracy of the simulations. Additionally, a two-way Analysis of Variance (ANOVA) was conducted to examine the effect of sphere size and position in the workspace on the overall distance from the target position.

5.3 Results

Basin of attraction simulations revealed that the static positions with their associated initial conditions and muscle activations acted as equilibrium points for the system. To determine if static positions acted similar to equilibrium positions, the principles of the posture-movement paradox in the Equilibrium Point Hypothesis were used to define equilibrium positions by the ability of the arm's internal stimulations to overcome external force deviations. According to the Equilibrium Point Hypothesis, equilibrium points are defined as the state where a field has zero force and opposing muscles are in a state of balance with each other, meaning that they are resistant to any external forces applied but can be manipulated by internal stimulations and activations. Since the muscle activations were able to return the arm to the initial position, it was determined that the initial conditions and muscle activations of the static positions acted as static equilibrium positions as defined by the Equilibrium Point Hypothesis.

The basin of attraction simulations revealed that a 15 cm basin of attraction exists around the static equilibrium positions, regardless of configuration of the joint position. To determine the size of the basin of attraction, basin of attraction simulations were performed for the same 20 static joint positions from the static holding simulations. The chosen static position, the ending positions obtained, and the distance between the two was calculated and recorded for a total of 52 points (13 points per sphere) for each static equilibrium position. Spheres of 5 cm, 10 cm, 15 cm, and 20 cm, and starting positions versus final positions for an arbitrary joint position can be seen in Figure 10 below. Results from these calculations determined that when the arm was moved to spheres up to 15 cm, muscle activations could adequately return the arm back to the original static equilibrium position, as seen in Figure 10(a). However, when the arm was moved to distances greater than 15 cm from the initial position, muscle activations were unable to overcome the distance and the arm could not adequately return to the static equilibrium position, as seen in Figure 10(b) below. For all 20 static positions, the averaged distance between the initial and final position when moving the arm to the individual spheres was calculated and can be seen in Figure 11. This data verified that muscle activations were successful at returning the arm to its initial position when moved to distances at or below 15 cm. Moving to distances above 15 cm, the arm was outside of the basin of attraction and muscle activations alone were not enough to overcome the distance. During simulations, it was noticed that when the arm was moved to a position on the 20 cm sphere below the target position, the muscle activations were unable to overcome the distance and gravitational forces, and the arm remained close to the position on the sphere. When the arm was moved to a position on the 20 cm sphere above the target position, the muscle activations moved the arm towards the direction of the target point, but the gravitational force and inadequacy of the muscle activations at further locations resulted in the ending position being lower than the target position. Therefore, we were able to limit the size of the basin of attraction to between 15 and 20 cm around the initial joint position, regardless of joint configuration, while using 15 cm as the more conservative estimate.

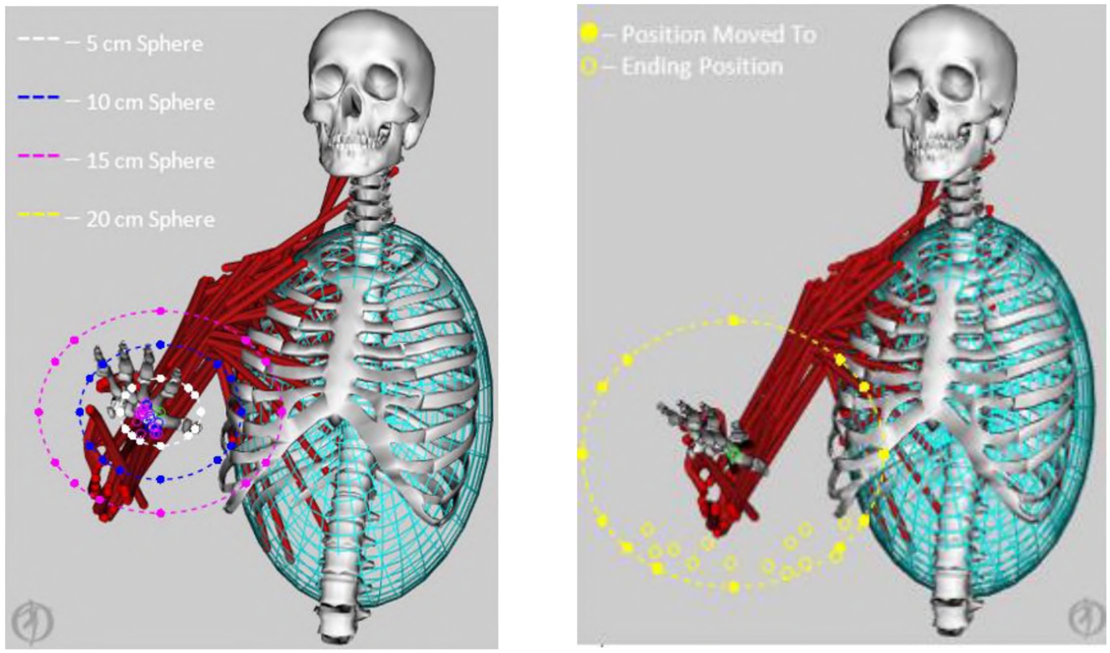

(a) Sphere Return Points of 5, 10, and 15 cm **(b) Sphere Return Points of 20 cm**

Figure 10 Basin of Attraction For an arbitrarily chosen joint position, the return points (open) for the 5 cm sphere (white), 10 cm sphere (blue), 15 cm sphere (pink), and 20 cm sphere (yellow) can be seen corresponding to the points on the basin they were initially moved to (closed). This verified that muscle activations were successful at returning the arm to position when moved up to 15 cm away

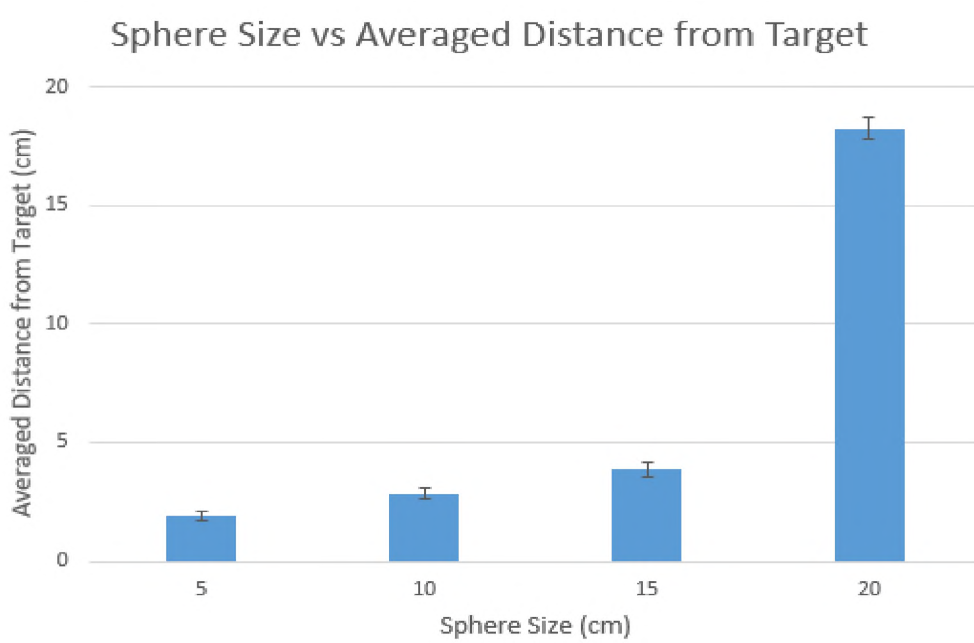

Figure 11 Sphere Averaged Return Data The averaged Euclidean distance was calculated for each sphere size for all 20 joint positions. It was found that, the farther an external force moved the arm away from the initial position, the greater the final distance from the initial position, up until it was completely unable to return the arm. The standard error of the mean was included for each group to show that it also increases with sphere size.

When examining arm movements during the simulations, it was noticed that the arm did return towards the original target position, but ended up at a different ending position area for each simulation. Although these ending positions were relatively close to the original positions for the 5, 10, and 15 cm basin sizes, it was interesting to note that the arm did not completely return to the original equilibrium position. An example of the movements of the arm coordinate positions over the course of the simulation can be seen in Figure 12 below for one arm position that was moved to points on the 5, 10, 15, and 20 cm spheres. These graphs show that the arm starts at the original equilibrium position and then is moved to coordinates of the particular sphere basin at 10 seconds. The external force is then removed at 15 seconds and the arm is given the rest of the simulation to return to the equilibrium position. It was apparent that as the arm was moved to the farther distanced spheres, the arm returned to ending positions further away from the original position, until it no longer adequately returned from the 20 cm sphere. These results could mean that there were multiple equilibrium positions for each simulation pattern, that there were undamped oscillations within the PD controller, that there was unaccounted for elasticity that is common in muscle models, or that implementing activations in a static model can potentially alter the static equilibrium position. The graphs identify that the simulations eventually settle out to an equilibrium point that is different, but relatively close, to the initial position, and future research will examine the exact cause of these results.

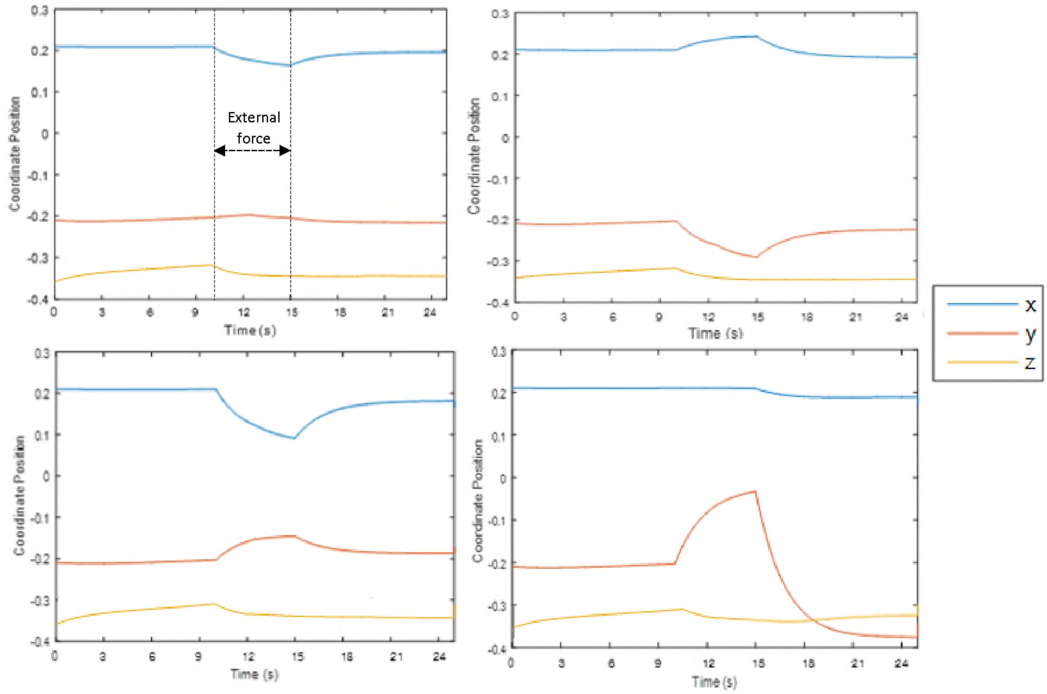

Figure 12 Coordinate Positions Over Time The graphs above show the X, Y, and Z coordinates of the arm over time for when the arm is moved from a target joint position to the 5 cm (top left), 10 cm (top right), 15 cm (bottom left), and 20 cm (bottom right) sphere groups with an external force. The external force is introduced at 10 seconds then removed at 15 seconds to allow the arm to move freely back towards the equilibrium position. The muscles are active during the entire time period.

It is worth noting that muscle activations could successfully discriminate between static equilibrium positions that were close together in the workspace. When the arm was moved into the basin of attraction for another position, muscle activations returned the arm to its initial position, instead of the alternative equilibrium position that was closer. This occurred regardless of location in the workspace or distance between the two discrete equilibrium positions. One example can be seen below in Figure 13. This verified that two-point discrimination exists in the system and that muscle activations can discern the difference between two nearby locations, illustrating that the initial conditions for the equilibrium point are specific to the position itself and the basin of attraction exists individually around each equilibrium point.

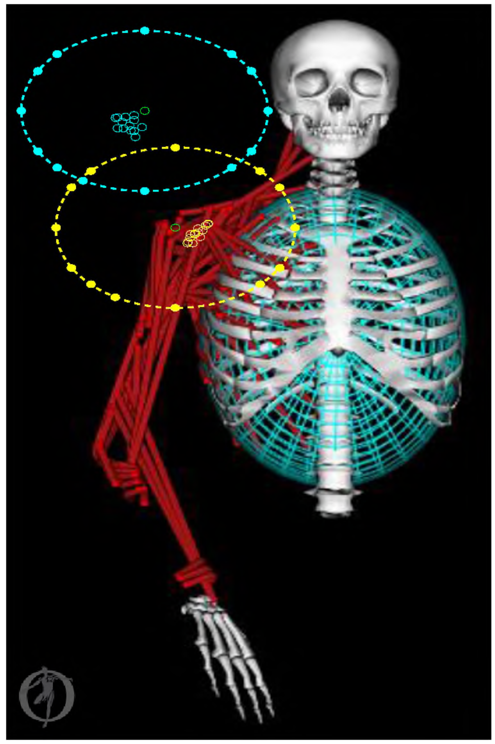

Figure 13 Point Discrimination Example of two target positions in the subject's workspace. The arm was moved to varying distances denoted by the filled points. When the arm was moved into a position occupied by another basin of attraction, muscle activations were able to return the arm to its initial static position as the muscle activations could successfully discriminate between positions with no concern whether the arm would be attracted to multiple equilibrium points from one set of muscle activations.

A two-way ANOVA was performed and determined that the size of the basin of attraction was the same irrespective of position in the workspace or joint configuration. Generally, a two-way ANOVA is conducted to conclude if there is an interaction between two independent variables on a dependent variable. In this research, the two-way ANOVA was used to determine what effect sphere size or position in the workspace, the independent variables, had on the overall capability of the muscle activations to return the arm to its original position (final Euclidean distance), the dependent variable. All 20 static positions in the workspace were tested alongside the four sphere groups (5 cm, 10 cm, 15 cm, and 20 cm), generating a statistically significant p score for the sphere size group ($p < .001$) compared to the position in workspace group ($p = .53$). This identified that sphere size had a significant effect on the Euclidean distance while the position in the workspace did not. To isolate the independent variable in the sphere group responsible for the significant interaction, a multiple comparison test was performed to compare individual independent variables within the sphere size group and can be seen in Table II below. From the multiple comparison test, it was determined that the 20 cm sphere size had the only significant effect on the final Euclidean distance, compared to the other sphere sizes. Utilizing the two-way ANOVA allowed for statistical verification that a basin of attraction up to 15 cm caused no statistical significance in the final Euclidean distance for all joint positions throughout the workspace while attempting to return from sphere sizes above this was statistically unfeasible.

Two-Way ANOVA Results	
Multiple Comparison	***p***
Between 5 and 10 cm Sphere Sizes	.95
Between 5 and 15 cm Sphere Sizes	.24
Between 5 and 20 cm Sphere Sizes	< .001
Between 10 and 15 cm Sphere Sizes	.85
Between 10 and 20 cm Sphere Sizes	< .001
Between 15 and 20 cm Sphere Sizes	< .001

Table II Multiple Comparison Test Two-Way ANOVA comparison to determine statistically significant interactions within the sphere size group

5.4 Discussion

To better understand the underlying dynamics of the initial conditions at a static position, an external disturbance was used to move the arm out of place to estimate basin of attraction and equilibrium point data. From the basin of attraction simulations, it was verified that the static positions with the determined initial conditions acted as equilibrium points as defined by the Equilibrium Point Hypothesis. Additionally, a 15 cm basin of attraction was found to exist around the static equilibrium positions that allows the muscle activations to return the arm to the initial position. The basin of attraction was limited to 15 cm, as when the arm was moved to distances beyond this, muscle activations did not return to the equilibrium position. These results were significant in that they expanded on previous research that only examined the capability of static holding and provided an identifiable space around static positions capable of returning the arm. Additionally, current research has successfully utilized the basin of attraction with FES to develop a controller for lower limb muscle groups to stabilize posture, showing that a control strategy is an effective method in FES subjects (Ruhbakhsh, 2015). In our research, it was noted that the basin of attraction simulations were performed on a computer-simulated human arm of predetermined weight and length. The simulations would have to be recalibrated with the measured weight and length of the specific patient to ideally recreate the simulations in a human patient. Identifying static positions as equilibrium points and determining the size of the basin of attraction determines how far the equilibrium points can be from each other to adequately achieve controlled arm movements between these points.

CHAPTER VI

POINT-TO-POINT SIMULATIONS

Simulating movement between equilibrium points is necessary in determining the feasibility of movement between static positions along a path. The previous chapters have demonstrated that muscle activations determined from a controller are capable of static arm holding within a 15 cm basin of attraction around a given joint position in the workspace. Static holding muscle activations and joint position basins of attraction are crucial on their own, but are unable to tell us anything about movement between static joint positions. To demonstrate movement between joint positions, information gathered from the static holding and basin of attraction simulations was used to simulate movement between static points along a full-arm path in Section 6.1. In Sections 6.2 and 6.3, the results from these simulations and detailed discussion will be examined. This chapter seeks to answer that if simulated movement between equilibrium points is feasible, can full-arm reaching be achieved by point-to-point tracking control?

6.1 Simulation Review

To demonstrate that moving between static equilibrium points is feasible, paths within the workspace were chosen and broken down into several equilibrium points along the path. For each equilibrium point along the path, the joint torques and muscle activations were determined from the method seen below in Figure 14. The Cartesian coordinates for the equilibrium position were chosen in the workspace and converted to the corresponding joint angles from the DAS. The two-part controller was then used on these joint angles to determine the corresponding joint torques and muscle activations required to maintain the given equilibrium position and was repeated for all equilibrium positions along the path. Two sets of simulations were performed to test the hypothesis that movements are achievable within the basin of attraction by: 1) simulating movement to an intermediate point between the starting and end position and 2) simulating movement between two points outside of the size of the basin of attraction. The accuracy of the simulations was determined from the distance between the final position obtained and the goal position of the path.

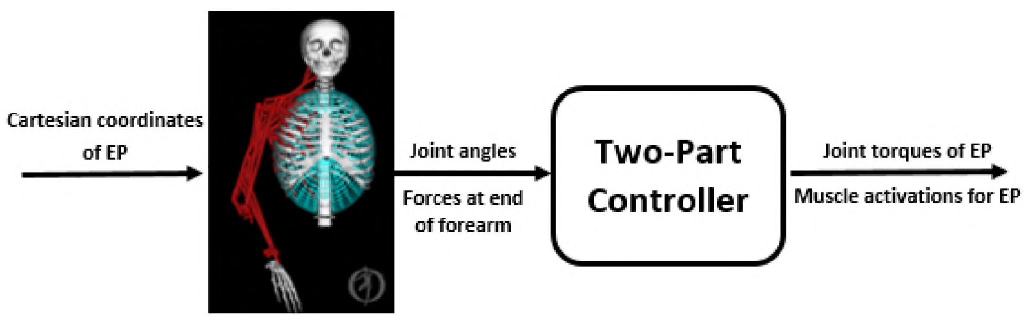

Figure 14 Determining Muscle Activations and Joint Torques Muscle activations and joint torques for the point-to-point stimulations were found from Cartesian coordinates of an equilibrium point in the DAS and manipulated through the controller

Point-to-point simulations between joint positions roughly 30 cm apart along a path were evaluated to determine if movements were feasible within the basin of attraction. The starting and end positions of a specific path were chosen that were outside of the respective basins of attraction. A third joint position roughly 10 to 15 cm away between the start and end path points was chosen to serve as the intermediate moving point. Muscle activations were found for each of the starting, intermediate, and ending joint positions using the process seen above Figure 14. Once the muscle activations for each position were found, an initial set of PD controller gains were used to move the arm to the starting joint position of the path while no muscles were activated. The PD controller was then shut off and the muscle activations for the starting position were input to allow activations to keep the arm static for 15 seconds. The simulated arm comes to equilibrium in 5 seconds, but was given 15 seconds for these simulations to completely settle into the equilibrium positions and minimize muscle perturbations. The muscle activations for the intermediate position then replaced the muscle activations for the starting position and were left in place for 15 seconds to allow the arm to move freely from the start position and settle into the intermediate position. Lastly, the muscle activations for the intermediate position were replaced with the muscle activations for the ending position, which were again left in place for 15 seconds to allow the arm to move freely from the intermediate position and settle into the ending goal position of the path. Once the PD controller was removed, muscle activations were the only stimuli allowed to move the arm from point-to-point. To estimate the accuracy of the simulations, the final position of the arm was recorded and the distance from the final position to the ending goal position was calculated. The simulation was repeated for 10 different paths, chosen from two of the static position points that were roughly 20 to 30 cm apart in the workspace, with an intermediate position being chosen for simulations within the basin of attraction. Some of the paths were chosen to simulate a variety of typical daily activities such as eating, grooming, and reaching to examine the performance of obtaining every day movements by starting in front of the body and ending near the face or hair.

Point-to-point simulations between joint positions roughly 20 cm apart along a path were evaluated to determine if these movements were feasible outside the basin of attraction. The starting and end positions for the paths above were chosen without using a third intermediate position. The path consisted of the starting and ending joint positions roughly 20 cm away from each other in the workspace to examine how the arm responds beyond the basin of attraction. Muscle activations were found for each of the joint positions using the process as seen above in Figure 14. Once the muscle activations for each position were found, an initial set of PD controller gains were used to move the arm to the starting joint position of the path while no muscles were activated. The PD controller was then shut off and the muscle activations for the starting position were input to allow activations to keep the arm static for 15 seconds. The above simulation was repeated for the start and ending joint positions without the intermediate transition position. To estimate the accuracy of the simulations, the final position of the arm was recorded and the distance from the final position to the ending goal position was calculated. The simulation was repeated for the same 10 paths as above but only separated into the starting and ending positions roughly 20 cm apart in the workspace.

6.2 Results

Point-to-point simulations revealed that arm movements between equilibrium points were feasible if distances remained within the basin of attraction. For simulations of distances within the basin of attraction, muscle activations were used to move the arm to joint positions approximately 10 to 15 cm apart, with the final positions being recorded for 10 separate paths. Comparing the distances between the final position obtained and the ending goal position for simulations within the basin of attraction, an averaged

Euclidean distance of 2.2$\pm$ 0.095 cm for all simulations was obtained. Majority of the arm movements in these simulations settled at distances physically below the ending goal position, possibly due to gravitational effects, but never fell short or overshot the targets, as seen in Figure 15 below. For simulations of distances outside the basin of attraction, muscle activations were used to move the arm to joint positions approximately 20 cm apart, with the final positions being recorded for 10 separate paths. Comparing the distances between the final position obtained and the ending goal position for simulations outside the basin of attraction, an averaged Euclidean distance of 18 $\pm$ 0.26 cm for all simulations was obtained. In these simulations, the muscle activations cause the arm to move slightly to attempt movement, but stays in place near the starting position of the path, which is akin to results from basin of attraction simulations in which the arm stayed at the edge of the 20 cm sphere size for a given equilibrium position. These results allow us to conclude that movements between static equilibrium positions is feasible for distances within the basin of attraction. The ability of muscle activations to move between static equilibrium points along a path from a starting position to a goal position demonstrates that full-arm reaching movements can be achieved using equilibrium point control.

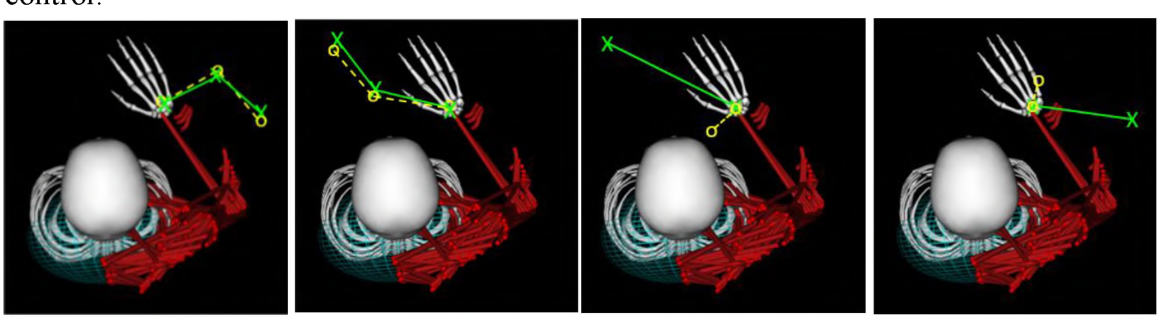

A **B** **C** **D**

Figure 15 Point-to-Point Simulations Comparisons between ideal arm movements along a path of equilibrium points with (A & B) and without (C & D) an intermediate point (green), and the observed arm movements along a path of obtained points (yellow)

6.3 Discussion

Point-to-point simulations were used to determine if movement between equilibrium points within the identified basin of attraction using muscle activations was feasible for full-arm trajectories. The hypothesis that full-arm reaching motions can be achieved through the transitioning of muscle activations between equilibrium points was successfully demonstrated by the ability of the muscle activations to navigate between discrete equilibrium points while remaining within 2.2 ± 0.095 cm standard deviation of the final goal without external assistance. Point-to-point simulations also showed that arm movements are only capable for distances within the basin of attraction as any attempts to move outside the basin of attraction left the arm close to its starting position at 18 ± 0.26 cm standard deviation from its goal. However, arm movements can start outside the basin of attraction for an equilibrium position, as long as there is an intermediate position to move to first before the desired equilibrium point. Point-to-point movements within the basin of attraction were found to be precise enough to perform detailed movements such as moving food to the patient's mouth or picking up smaller foods. Movements with less precision would be sufficient for tasks that do not require fine movements, but would perform poorly when tasked with movements that are more specific. Point-to-point simulations verified that movement along a path between static equilibrium positions composing full-arm reaching is possible throughout the workspace. These results also coincide with the underlying principles of the Equilibrium Point Hypothesis in that movement along a path is feasible when transitioning between equilibrium points. The addition we personally noted was that these movements were feasible as long as they occurred at distances within the basin of attraction of transitioning equilibrium points. It was of interest to note that the simulations performed point-to-point movements by direct control of muscles without access to a higher brain, in contrast to the need for motor innervation from a higher source in the Equilibrium Point Hypothesis principle of motor innervation. Despite the success of the findings, one of the limitations of these simulations were that they focused only on equilibrium points roughly 10 to 15 cm apart and 20 cm apart in the workspace. Future simulations could evaluate a broader range of distances to examine the accuracy of the arm to perform even more position-sensitive movements such as eating or drinking. Additionally, in these simulations, the arm was given 15 seconds between each position to settle into place. This is much longer than the 5 seconds necessary for the arm to settle and was used to give the arm extra time to remove any potential perturbations. Future simulations will reduce this settling time to achieve a more realistic timing of human arm movements. In these simulations, our findings determined that transitioning between equilibrium points along a path via the activation of various muscle groups is successful and capable of full-arm reaching movements in a simulated human arm.

CHAPTER VII

CONCLUSION

In this study, full-arm reaching movements were achieved between static equilibrium points using identified muscle activations. A virtual human arm model generated in Matlab and visually represented in OpenSim was used to simulate a human right arm with a predetermined length and weight. External forces were used to hold the arm in place while internal activations were used to mimic the activation of various muscle groups. Simulations were performed to identify a two-part controller with GPR models capable of calculating muscle activations required to maintain desired joint positions in the workspace. Once the static holding of joint positions was achieved, simulations were performed to define static positions as equilibrium points and to estimate the size of the basin of attraction. Simulations performed in this research identified that equilibrium point control of full-arm motions was achievable for reaching paths throughout the workspace.

Simulations performed identified three significant findings regarding the underlying properties of human arm movement, while also acknowledging research limitations. First, the identification of a virtual model allowed for the development of a two-part controller with GPR models capable of successfully holding static joint positions in the workspace. This finding agreed with current research that has developed a controller capable of identifying muscle group stimulations for holding a human arm in position with a FES neuroprosthesis (Wolf, 2017). Second, the static positions were identified as equilibrium positions for a set of initial conditions as they could return the arm to the initial position when the arm was moved away by an external force. Third, basin of attraction simulations identified that a 15 cm basin of attraction exists around each equilibrium position. Within the basin of attraction, muscle activations could return the arm back to the initial equilibrium position, irrespective of position in the workspace. Identifying equilibrium points and basin of attraction size allowed point-to-point movements to be examined by separating distant paths into manageable equilibrium points within the basins of attraction. In our research, a computer-simulated human arm model was used in place a patient with an implanted FES, limiting the research to strictly virtual models. However, the virtual model allowed more simulations to be conducted as muscle fatigue or limited patient time would not occur. The weight and length of the virtual arm was obtained from cadaver studies and was used to determine the feasibility of our hypothesis. Once the arm data of a patient has been identified, the controller can be recalibrated and repeated with these measurements to allow for patient-specific joint data and to verify if the size of the basin of attraction is consistent among arm measurements. The success of these simulations supported the Equilibrium Point Hypothesis in that full-arm movements are feasible between equilibrium points. Despite the limitations in this research, the findings have demonstrated that arm movement utilizing muscle stimulations is controllable can be achieved for full-arm reaching throughout an identified workspace.

Current researched focused on FES has made great strides in upper limb movement in high-level tetraplegia, but still lacks the ability for complete mobility and independence. One current human research study has demonstrated that muscle stimulations for a specified joint position can be generated from a controller using a human subject with high-level tetraplegia as the model (Wolf, 2017). In both this research and ours, a controller was developed capable of generating muscle activations to hold an arm in a specified joint position. However, the human subject could only achieve static holding with the aid of a robotic arm, whereas simulations performed in our research were capable of movement within a reasonably small basin of attraction. Other FES research trials have shown promise in successful muscle or nerve stimulation or potential full-arm movement (Ajiboye, 2017; Pedrocchi, 2013; Ho, 2014). However, these research trials lack effective control methods for upper limb movements as they focused on a single joint aided by arm support. Our research presented a more general method of control for upper limb movement by developing a controller capable of determining muscle activations for movement between equilibrium points.

The potential for FES technology to allow high-level tetraplegia patients to regain some level of mobility in their upper limbs gives them a greater chance at leading a more normal and independent lifestyle. The findings in this research aim to improve the current methods – Braingate and MUNDUS - available to high-level tetraplegia patients and provide them with a potential functional method of obtaining upper-limb movements. Future research aims to identify the physical arm data of a high-level tetraplegia patient to recalibrate the two-part controller. The controller can then be used to implement muscle activation data for an identified human patient. Adding a third block to the controller to convert muscle activations into corresponding muscle stimulations would allow them to be utilized by an implanted FES neuroprosthesis. The simulations can then be performed to attempt to recreate the simulations in a human arm patient. The research presented in this thesis can provide much needed full-arm reaching movements to high-level tetraplegia patients, which is currently lacking by current research methods present today.

BIBLIOGRAPHY

1. Ajiboye, A. et al. "Restoration of Reaching and Grasping Movements through Brain-Controlled Muscle Stimulation in a Person with Tetraplegia: A Proof-of-Concept Demonstration." *The Lancet* 389.10081 (2017): 1821–1830. Web.
2. Archambault, P.S. et al. "Basic Elements of Arm Postural Control Analyzed by Unloading." *Experimental Brain Research* 164.2 (2005): 225-241. Web.
3. An, K. et al. "Internal Features in Basin of Attraction of the Simplest Walking Model." *Journal of Mechanical Science and Technology* 29.11 (2015): 4913–4921. Web.
4. Anderson, K. "Targeting Recovery: Priorities of the Spinal Cord-Injured Population." *Journal of Neurotrauma* 21.10 (2004): 1371-1383. Web.
5. Byeong-Sang, K. et al. "Equilibrium Point Control of a Robot Manipulator Using Biologically-Inspired Redundant Actuation System." *Advanced Robotics* 27.8 (2013): 567-579. Web.
6. Chadwick, E. et al. "Real-Time Simulation of Three-Dimensional Shoulder Girdle and Arm Dynamics." *IEEE Transactions on Biomedical Engineering* 61.7 (2014): 1947–1956. Web.
7. Esquenazi, A. et al. "The ReWalk Powered Exoskeleton to Restore Ambulatory Function to Individuals with Thoracic-Level Motor-Complete Spinal Cord Injury." *American Journal of Physical Medicine & Rehabilitation* 91.11 (2012): 911–921. Web.
8. Feldman, A. "Once More on the Equilibrium-Point Hypothesis (λ Model) for Motor Control." *Journal of Motor Behavior* 18.1 (1986): 17–54. Web.

9. Feldman, A., and Ostry, D. "A Critical Evaluation of the Force Control Hypothesis in Motor Control." *Experimental Brain Research* 153.3 (2003):275-288. Web.
10. Feldman, A., and Latash, M. "Testing Hypotheses and the Advancement of Science: Recent Attempts to Falsify the Equilibrium Point Hypothesis." *Experimental Brain Research* 161.1 (2005): 91–103.Web.
11. Feldman, A., and Levin, M. "The Equilibrium-Point Hypothesis – Past, Present and Future." *Progress in Motor Control* (2009): 699–726.Web.
12. Gu, X., and Ballard, D. "An Equilibrium Point Based Model Unifying Movement Control in Humanoids." *Robotics: Science and Systems* 7.2 (2007): 129-135. Web.
13. Ho, C. et al. "Functional Electrical Stimulation and Spinal Cord Injury." *Physical medicine and rehabilitation clinics of North America* 25.3 (2014): 631–ix. Web.
14. Jarosz, R. et al. "Functional Electrical Stimulation in Spinal Cord Injury Respiratory Care." *Topics in Spinal Cord Injury Rehabilitation* 18.4 (2012): 315–321. Web.
15. Keith, M. W. et al. "Tendon Transfers and Functional Electrical Stimulation for Restoration of Hand Function in Spinal Cord Injury." *The Journal of Hand Surgery* 21.1 (1996): 89–99. Print.
16. Memberg, W. D. et al. "Implanted Neuroprosthesis for Restoring Arm and Hand Function in People with High-Level Tetraplegia." *Archives of Physical Medicine and Rehabilitation* 95.6 (2014): 1201–1211. Web.
17. Monohar, V. et al. "Limits of the Dual-Strategy Hypothesis in an Isometric Plantar Flexion Contraction." *Experiment Brain Research* 122.4 (1998): 459-466. Web.
18. Murphy, K. "Machine Learning: A Probabilistic Perspective." *The MIT Press* (2012): 492-493. Web.

19. National Spinal Cord Injury Statistical Center, "Spinal Cord Injury Facts and Figures at a Glance." *The Journal of Spinal Cord Medicine* 35.4 (2017): 197–198. Web.

20. Nielsen, M. "Neural Networks and Deep Learning." *Determination Press* (2015). Web.

21. Pedrocchi, A., Ferrante, S., et al. "MUNDUS project: Multimodal Neuroprosthesis for daily Upper limb Support." *Journal of NeuroEngineering and Rehabilitation* (2013): 10:66. Web.

22. Quandt, Fanny, and Hummel, F. "The Influence of Functional Electrical Stimulation on Hand Motor Recovery in Stroke Patients: A Review." *Experimental & Translational Stroke Medicine* 6 (2014): 9. Web.

23. Ragnarsson, K. T. "Functional Electrical Stimulation after Spinal Cord Injury: Current Use, Therapeutic Effects, and Future Directions." *Spinal Cord* 46.4 (2008): 255–274. Web.

24. Rasmussen, C. E., and Williams, C. "Gaussian Processes for Machine Learning." *University Press Group Limited* (2006). Web.

25. Ruhbakhsh, S., and Kobravi, H. "Preserving Balance During Unsupported Standing Using Synergistic Combination of Discrete Sliding Predictive and Adaptive Controllers." *International Congress on Technology, Communication and Knowledge* (2015). Web.

26. Sainburg, R. L. "Should the Equilibrium Point Hypothesis (EPH) Be Considered a Scientific Theory?" *Motor Control* 19.2 (2015): 142–148. Web.

27. Schearer, E. M., Wolf, D. N., and Kirsch, R. F. “Quasi-Static Control of Whole-Arm Motions with FES.” *Converging Clinical and Engineering Research on Neurorehabilitation II* (2017): 673–677. Web.

28. Schearer, E. M. et al. “Identifying Inverse Human Arm Dynamics Using a Robotic Testbed.” *International Conference on Intelligent Robots and Systems* (2014). Web.

29. Shadmehr, R. et al. “Postural Force Fields of the Human Arm and Their Role in Generating Multijoint Movements.” *Journal of Neuroscience* 13.1 (1993): 45-62. Web.

30. Sullivan, L. “Power and Sample Size Determination.” *Issues in Estimating Sample Size for Confidence Intervals Estimates* (2017) Web.

31. Todorov, E. “Probabilistic Inference of Multijoint Movements, Skeletal Parameters and Marker Attachments from Diverse Motion Capture Data.” *IEEE Transactions on Biomedical Engineering* 54.11 (2007): 1927–1939. Web.

32. Wolf, D., and Schearer, E. M. “Evaluating an Open-Loop Functional Electrical Stimulation Controller for Holding the Shoulder and Elbow Configuration of a Paralyzed Arm.” *IEEE International Conference on Rehabilitation Robotics* (2017): 789-794. Web.

33. Wu, G. et al. "ISB Recommendation on Definitions of Joint Coordinate Systems of Various Joints for the Reporting of Human Joint motion—Part II: Shoulder, Elbow, Wrist, and Hand." *Journal of Biomechanics* 38.5 (2005): 981–992. Web.

34. Zhang, D., and Zhu, K. “Modeling Biological Motor Control for Human Locomotion with Functional Electrical Stimulation.” *Biological Cybernetics* 96.1 (2007): 79–97. Web.